Development 138, 5291-5300 (2011) doi:10.1242/dev.067470

Six3 is required for ependymal cell maturation

Alfonso Lavado and Guillermo Oliver*

SUMMARY

Ependymal cells are part of the neurogenic niche in the adult subventricular zone of the lateral ventricles, where they regulate neurogenesis and neuroblast migration. Ependymal cells are generated from radial glia cells during embryonic brain development and acquire their final characteristics postnatally. The homeobox gene *Six3* is expressed in ependymal cells during the formation of the lateral wall of the lateral ventricles in the brain. Here, we show that Six3 is necessary for ependymal cell maturation during postnatal stages of brain development. In its absence, ependymal cells fail to suppress radial glia characteristics, resulting in a defective lateral wall, abnormal neuroblast migration and differentiation, and hydrocephaly.

KEY WORDS: Subventricular zone, Ependymal cells, Six3, Mouse

INTRODUCTION

The subventricular zone (SVZ) of the lateral ventricles is one of the neurogenic niches in the adult mouse brain (Alvarez-Buylla and Garcia-Verdugo, 2002; Doetsch and Alvarez-Buylla, 1996; Miller and Gauthier-Fisher, 2009). The SVZ generates neuroblasts that migrate to the olfactory bulb (OB) and differentiate into olfactory interneurons during adult stages (Lois and Alvarez-Buylla, 1994) and is composed of astrocyte-like neural stem cells (aNSCs), neuroblasts, blood vessels and ependymal cells (Alvarez-Buylla and Lim, 2004; Doetsch, 2003; Miller and Gauthier-Fisher, 2009; Shen et al., 2008; Tavazoie et al., 2008).

Ependymal cells are neuroepithelial multi-ciliated cells that form a continuous single-cell layer that lines the lateral ventricles (LVs) (Doetsch et al., 1997). Ependymal cells regulate neurogenesis in the SVZ by several mechanisms; for example, they secrete the bone morphogenetic protein (BMP) inhibitor noggin, thereby inducing neurogenesis and suppressing gliogenesis (Chmielnicki et al., 2004; Lim et al., 2000). Ependymal cells are also a source of pigment epithelium-derived factor, which promotes self-renewal of aNSCs (Ramírez-Castillejo et al., 2006). The beating motion of ependymal cilia is required for normal cerebrospinal fluid flow and neuroblast migration towards the OB (Sawamoto et al., 2006). Under normal conditions, forebrain ependymal cells are quiescent; however, they can acquire radial glia characteristics and give rise to neuroblasts and astrocytes in response to stroke (Carlén et al., 2009; Zhang et al., 2007).

Ependymal cells are generated from radial glia during embryonic brain development and acquire their final characteristics postnatally (Spassky et al., 2005). The mechanisms that control ependymal cell maturation have been poorly characterized. However, it is known that the forkhead transcription factor FoxJ1 is necessary for ependymal cell maturation and ciliogenesis (Jacquet et al., 2009; Yu et al., 2008).

The homeobox gene *Six3* is expressed in the mouse anterior neural plate around embryonic day (E) 7.5. Later, *Six3* is expressed in the anterior neuroectoderm, presumptive eye field, basal ganglia, prethalamus, hypothalamus and pituitary (Conte et al., 2005; Oliver et al., 1995). Early during development, *Six3* maintains anterior forebrain identity and is required for neuroretinal specification (Geng et al., 2008; Lagutin et al., 2003; Lavado et al., 2008; Liu et al., 2010). However, the functional roles of Six3 during later stages of brain development remain unknown.

Here, we report that Six3 is expressed in ependymal cells during the formation of the lateral wall of the LV (LW) and that conditional inactivation of *Six3* at later stages of brain development results in abnormal ependymal cell maturation. Consequently, the cells lining the LV have mixed ependymal and radial glia features. This results in damage to the LW, abnormal neuroblast migration and differentiation, and hydrocephaly.

MATERIALS AND METHODS

Mice

Six3$^{+/-}$ (Lagutin et al., 2003), *Six3*$^{f/f}$ (Liu et al., 2006), *Nestin-Cre* (Betz et al., 1996) and *Nestin-CreER*^{T2} (Cicero et al., 2009) mice have been described previously. Tamoxifen (Sigma, St Louis, MO, USA) was dissolved in oil at 20 mg/ml. To induce Cre recombination, pups were given injections of tamoxifen (4 mg/20 g body weight) twice between postnatal day (P) 0 and P5. *Nestin-Cre;Six3*$^{f/+}$ and *Nestin-CreER*^{T2}*;Six3*$^{f/+}$ mice were used as controls.

In situ hybridization

In situ hybridization was performed as previously described (Schaeren-Wiemers and Gerfin-Moser, 1993). Probes were used against *Dlx2* and *Lhx2* (J. L. Rubenstein, UCSF, San Francisco, CA, USA), and *Ttr* (S. Aizawa, RIKEN, Kobe, Japan).

Immunohistochemistry

Immunohistochemistry (IHC) was performed on cryostat sections (Lavado and Oliver, 2007). For whole-mount IHC, tissue was permeabilized in PBS and 0.01% Triton X-100 for 30 minutes; primary and secondary antibodies were incubated overnight at room temperature (RT) in 2% fetal calf serum (FCS) and 0.01% Triton X-100 in PBS. The following antibodies and dilutions were used: rabbit anti-β-Gal (1:1000; ICN, Aurora, OH, USA), chicken anti-β-Gal (1:1000; Abcam, Cambridge, MA, USA), mouse anti-Ascl1 (1:100; BD Pharmingen, San Diego, CA, USA), mouse anti-S100β (1:100; Sigma, St Louis, MO, USA), guinea pig anti-vimentin (1:1000; RDI, Acton, MA, USA), rabbit anti-Gfap (1:1000; Sigma), mouse anti-Gfap (1:1000; Sigma), goat anti-nestin (1:100; R&D, Minneapolis, MN, USA), rabbit anti-Blbp (1:200, Millipore, Billerica, MA, USA), rat anti-CD31 (1:1000; BD Pharmingen), rabbit anti-acetylated tubulin (1:1000; Sigma), rabbit anti-γ-tubulin (1:1000; Sigma), rabbit anti-Dcx (1:1000; Millipore), goat anti-Dcx (1:500; Santa Cruz Biotechnology, Santa Cruz,

Department of Genetics, St. Jude Children's Research Hospital, 262 Danny Thomas Place, Memphis, TN 38105, USA.

*Author for correspondence (guillermo.oliver@stjude.org)

Accepted 12 October 2011

CA, USA), guinea pig anti-Glast (1:5000; Millipore), mouse anti-βTub-III (1:500; BabCO, Richmond, CA, USA), rat anti-noggin (1:500; a gift from Aris Economides, Regeneron Pharmaceuticals, Tarrytown, NY, USA), rabbit anti-Numb/Numbl (1:1000; a gift from K. Zuo, Yale University, New Haven, CT, USA), Alexa-488-anti-Phalloidin (1:20; Invitrogen, Carlsbad, CA, USA), rabbit anti-Ng2 (Millipore; 1:1000), rabbit anti-Olig2 (1:40,000; a gift from C. Stiles, Harvard Medical School, Boston, MA, USA), rabbit anti-Six3 (1:500; our own) and guinea pig anti-Six3 (1:100; our own). The guinea pig anti-Six3 was generated in Rockland using a KLH-conjugated peptide against the internal region of Six3. The sequence of the peptide was RLQHQAIGPSGMRSLAEPGC. The secondary antibodies used were from Molecular Probes or Jackson ImmunoResearch (West Grove, PA, USA): anti-rabbit, anti-chicken, anti-mouse, anti–guinea pig, anti-rat or anti-goat Alexa 488, Alexa 594 and Cy3. Low-magnification images were obtained using a Leica MZFLIII stereomicroscope equipped with a Hanamatsu C5810 camera and a Zeiss Axiovert 1.0 microscope equipped with a ProgRes C14 camera. Area measurements were obtained using ImageJ software. The remaining images were obtained with a Leica SP1 or a Zeiss LSM 510 NLO Meta confocal microscope. Whole-mount IHC three-dimensional pictures were processed using Imaris software.

Quantification and statistical analysis

For the number of positive cells, ten consecutive coronal sections at a similar level of the anteroposterior axis were analyzed per specimen. Typically, comparisons were made in sections taken after the corpus callosum crossed the midline but before the anterior commissure appeared ventrally. Positive cells were quantified in both brain hemispheres along the striatal side of the SVZ dorsoventral axis. An average value per section/specimen was obtained; the average value ± s.d. from at least three specimens was represented in the graphs. Comparisons were made using a paired *t*-test.

For the percentage of cells that were also positive for another marker, we quantified the number of positive cells following the above criteria. The percentage of cells of a particular population that were also positive for another marker was calculated for each section. An average value per section was obtained for each specimen. The average value ± s.d. from at least three specimens was represented in the graphs. Comparisons were made using a paired *t*-test.

For quantification of the LV and SVZ areas, images from ten consecutive coronal sections at a similar level of the anteroposterior axis were taken per specimen. Relative area values along the dorsoventral axis were obtained with ImageJ64 software. A similar value was obtained for the total area of the section. An LV or SVZ area versus total area of the section ratio was obtained per section. An average value per section for each specimen was obtained; the average value ± s.d. for at least three specimens was represented in the graphs. Comparisons were made using a paired *t*-test.

Electron microscopic analysis

Electron microscopy was performed at the St. Jude Electron Microscopy Facility. P20 brains were perfused in 4% paraformaldehyde (PFA) and post-fixed in 2.5% glutaraldehyde in 0.1 M sodium cacodylate buffer. The samples were post-fixed in 2% osmium tetroxide and dehydrated via a graded series of alcohol, cleared in propylene oxide, embedded in epon araldite and polymerized overnight at 70°C. Sections (70 nm thick) were cut on a Leica Ultracut E. The unstained sections were imaged on a JEOL 1200 EX Transmission Electron Microscope with an AMT 2K digital camera.

TUNEL and proliferation assays

TUNEL assays were performed on tissue sections as previously described (Lavado et al., 2008). For proliferation assays, pups were given injections of with BrdU (100 μg/g body weight, intraperitoneally), and brains were collected 1 hour later. BrdU incorporation was exposed after 20 minutes treatment in 2 N HCl. Mouse anti-BrdU (1:10; BD Pharmingen) and rat anti-BrdU (1:1000; Accurate Biochemicals, Westbury, NY, USA) antibodies were used.

Neurosphere cultures and immunocytochemistry

Neurosphere cultures were established as described, with modifications (Reynolds and Weiss, 1992). Briefly, P7 SVZs were dissected, disaggregated in trypsin and maintained in neurosphere culture medium (Neurobasal medium with GlutaMAX, Pen/Strep, B27 and N2; Invitrogen) supplemented with 20 ng/ml epidermal growth factor (Upstate Biotechnology, Waltham, MA, USA) and 20 ng/ml fibroblast growth factor (Millipore). After the third passage, neurospheres were differentiated for 4 days in neurosphere culture medium with 10% FCS without supplements on Lab-Tek II CC^2 chamber slides (Nalge Nunc International, Rochester, NY, USA). Cells were fixed in 2% PFA for 15 minutes at RT. Cells were blocked in 10% FCS for 30 minutes at RT and incubated with the appropriate primary and secondary antibodies (see above) in 2% FCS for 2 hours.

Primary neurosphere quantification was performed in cultures established from P7 SVZs as described above. After disaggregation, cells were plated at a density of 20,000 cells/ml in 24-well plates and maintained in neurosphere culture medium as described above. After 7 days, the number of neurospheres per well was counted. Neurosphere cultures from three specimens per genotype were analyzed, and 24 wells from each genotype were quantified. An average number of neurospheres per well for each specimen was calculated, and the average ± s.d. of the three specimens per genotype was represented. Comparisons were made using a paired *t*-test.

RESULTS

Six3 is expressed in ependymal cells during the formation of the lateral wall

To identify possible functional roles of Six3 during later stages of brain development, we compared its expression pattern in P4 and P15 brains with that of the astrocyte marker Gfap, the progenitor marker Ascl1, the immature neuronal marker Dcx, the immature oligodendrocyte markers Olig2 and Ng2 (Cspg4 – Mouse Genome Informatics), the forkhead gene FoxJ1 and the ependymal cell marker vimentin. We took advantage of a *Six3* allele in which *lacZ* cDNA was inserted in frame into the *Six3* locus (Lagutin et al., 2003). This allele fully recapitulates the Six3 expression pattern; $Six3^{+/-}$ mice are indistinguishable from wild-type mice (Lagutin et al., 2003; Lavado et al., 2008). We found that at these stages, Six3 was expressed in $FoxJ1^+$ (supplementary material Fig. S1F,M) and $vimentin^+$ (supplementary material Fig. S1G,N) cells lining the LV during LW formation, but not in $Gfap^+$ (supplementary material Fig. S1A,H), $Ascl1^+$ (supplementary material Fig. S1B,I), Dcx^+ (supplementary material Fig. S1C,J), $Olig2^+$ (supplementary material Fig. S1D,K) or $Ng2^+$ (supplementary material Fig. S1E,L) cells. This suggests that Six3 is involved in the maturation of ependymal cells. To characterize further the expression pattern of Six3 at these stages, we compared its expression profile with that of Glast (Slc1a3 – Mouse Genome Informatics), vimentin and S100β. Glast is a radial glia marker that during later development is expressed in astrocytes and neuroblasts; however, it is absent from ependymal cells (Shibata et al., 1997). At P4, most of the cells lining the striatal side of the LV were $Glast^+$ (Fig. 1D). As some radial glia matured into ependymal cells, the number of $Glast^+$ cells lining the striatal side of the LV decreased (Fig. 1E). By P15, when the LW is nearly formed (Spassky et al., 2005), most cells lining the LV were $Glast^-$ (Fig. 1F). Next, we compared this expression with that of Six3. During the formation of the LW, Six3 was not expressed in $Glast^+$ cells at any of the analyzed stages (Fig. 1D′-F′), indicating that Six3 is not expressed in postnatal radial glia, astrocytes or neuroblasts.

In contrast to Glast, vimentin is expressed by radial fibers during embryonic development and in ependymal cells at adult stages (Mirzadeh et al., 2008; Schnitzer et al., 1981). At P4, vimentin expression was detected on some cells lining the striatal side of the LV (Fig. 1G). Most of the cells in the LW at P7 and P15 were

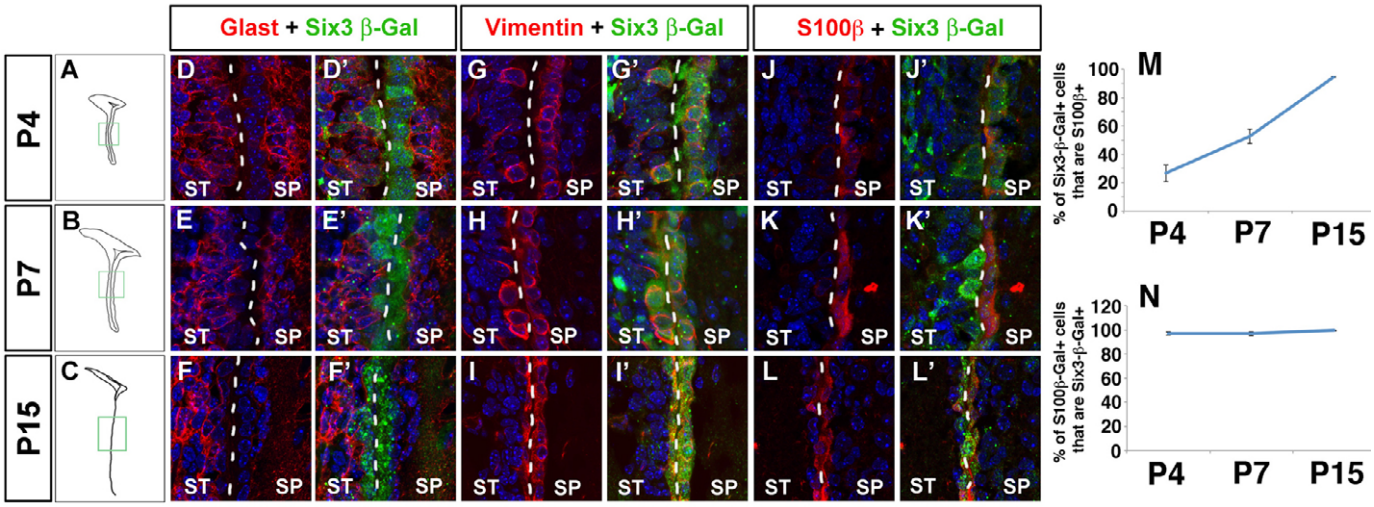

Fig. 1. Six3 is expressed in ependymal cells during the formation of the lateral wall of the lateral ventricles. (**A-C**) Diagrams depict the dorsoventral axis level of the LW at which the high-magnification pictures were taken in controls at P4 (A), P7 (B) and P15 (C). (**D-L′**) As shown by Six3-β-Gal/Glast staining, Six3 was not expressed in Glast$^+$ cells during LW formation at P4 (D,D′), P7 (E,E′) or P15 (F,F′). However, Six3 was expressed in vimentin$^+$ (G-I′) and S100β$^+$ (J-L′) cells at P4, P7 and P15. (**M**) Furthermore, the percentage of Six3-β-Gal$^+$ cells that were also S100β$^+$ increased as the formation of the LW progressed from P4 to P15. Data represent the mean of the percentage of Six3-β-Gal$^+$ cells that are also S100β$^+$ per section per pup ± s.d. (**N**) Moreover, nearly all the S100β$^+$ cells were Six3-β-Gal$^+$ at these stages. Data represent the mean of the percentage of S100β$^+$ cells that were also Six3-β-Gal$^+$ per section per pup ± s.d. *n*=3 pups. The dashed line shows the location of the lateral ventricles. ST, striatum; SP, septum.

vimentin$^+$ (Fig. 1H,I). Similar expression was observed using the ependymal cell marker S100β (Didier et al., 1986) (Fig. 1J,K,L). Six3 expression overlapped with that of vimentin (Fig. 1G′-I′) and S100β (Fig. 1J′-L′) at all stages. As the formation of the LW progressed, the percentage of Six3-β-Gal$^+$ cells lining the striatal side of the LV that were also S100β$^+$ increased (Fig. 1M). Nearly 100% of S100β$^+$ cells were also Six3-β-Gal$^+$ at P4, P7 and P15 (Fig. 1N). Double labeling of cells with Six3 and S100β (Fig. 3A,B) confirmed that Six3 is expressed in ependymal cells during the formation of the LW.

The ependymal lateral wall is defective in Nestin-Cre;Six3$^{f/-}$ mice

We previously reported that *Six3*-null embryos lack most of the forebrain and die soon after birth (Lagutin et al., 2003; Lavado et al., 2008). Accordingly, to identify possible functional roles of Six3 in the formation of the LW, we used a conditional inactivation approach. *Six3*$^{+/-}$ mice (Lagutin et al., 2003) were bred with *Nestin-Cre* mice, in which constitutively active Cre is expressed in neural progenitors from E10.5 (Betz et al., 1996). Then, *Nestin-Cre;Six3*$^{+/-}$ animals were crossed with a *Six3*-floxed strain (*Six3*$^{f/f}$) (Liu et al., 2006) to generate *Nestin-Cre;Six3*$^{f/-}$ mice. This strategy was used to obtain *Six3*-conditional mutants with the maximum deletion efficiency. Consequently, no vimentin$^+$Six3$^+$ cells remained in the LW in *Nestin-Cre;Six3*$^{f/-}$ brain (supplementary material Fig. S2A,B)

An initial characterization of the anterior telencephalon of P0 *Nestin-Cre;Six3*$^{f/-}$ pups using the telencephalic markers *Dlx2* (Porteus et al., 1991) and *Lhx2* (Porter et al., 1997) (supplementary material Fig. S3A-H) revealed no obvious alterations in the brain. However, the SVZ (Fig. 2A-C) and LV (Fig. 2A,B,D) appeared to be enlarged in the mutant brain at P7 and P15. A more detailed analysis of these alterations using Hematoxylin and Eosin (HE) staining and S100β revealed that the integrity of the LW was severely disrupted in the mutants at P15 (Fig. 2E-H). Whole-mount S100β IHC revealed that some areas of the LW (Fig. 2I,J) and the medial wall (not shown) of P15 *Nestin-Cre;Six3*$^{f/-}$ pups were devoid of S100β$^+$ cells. A detailed quantification showed that fewer S100β$^+$ cells were present in the LW at P4, P7 and P15 (Fig. 2K).

F-actin is expressed in the apical borders of the LW of P7 wild-type animals. Expression of F-actin and E-cadherin is lost in the absence of Numb/Numbl activity (Kuo et al., 2006). We found that in P7 *Nestin-Cre;Six3*$^{f/-}$ pups, the number of cells expressing F-actin in the apical border of the LW was substantially reduced and discontinuous; instead, F-actin was expressed by cells without contact with the LV (supplementary material Fig. S4A,C). Moreover, the expression of Numb/Numbl was not obviously affected in the S100β$^+$ cells of the mutants (supplementary material Fig. S4D,E). This indicates that conditional removal of Six3 results in a defective LW; however, this defect is not Numb/Numbl-dependent. Together, these findings suggest that Six3 activity is required during some steps leading to the formation of the LW.

Six3 is necessary for the transition of radial glia to ependymal cells

As shown above, Six3 is expressed in S100β$^+$ cells during LW formation, and in the absence of Six3, the number of these cells is reduced (Fig. 2K). To determine whether this reduction is due to a role of Six3 in radial glia pre-natally or in ependymal cell formation postnatally, we compared the expression pattern of Six3 in the basal telencephalon with that of nestin and β-Tub-III at E12.5, E14.5, E16.5 and P0. We found that from E12.5 onwards, Six3 was expressed only in Nestin$^-$β-Tub-III$^+$ cells (supplementary material Fig. S5A-H). This indicates that the reduction in the number of S100β$^+$ cells in *Nestin-Cre;Six3*$^{f/-}$ pups is not because of a role of Six3 in radial glia cells pre-natally.

To determine whether Six3 is necessary for the formation or survival of ependymal cells at later stages, we investigated whether its conditional inactivation affects the maturation of radial glia into

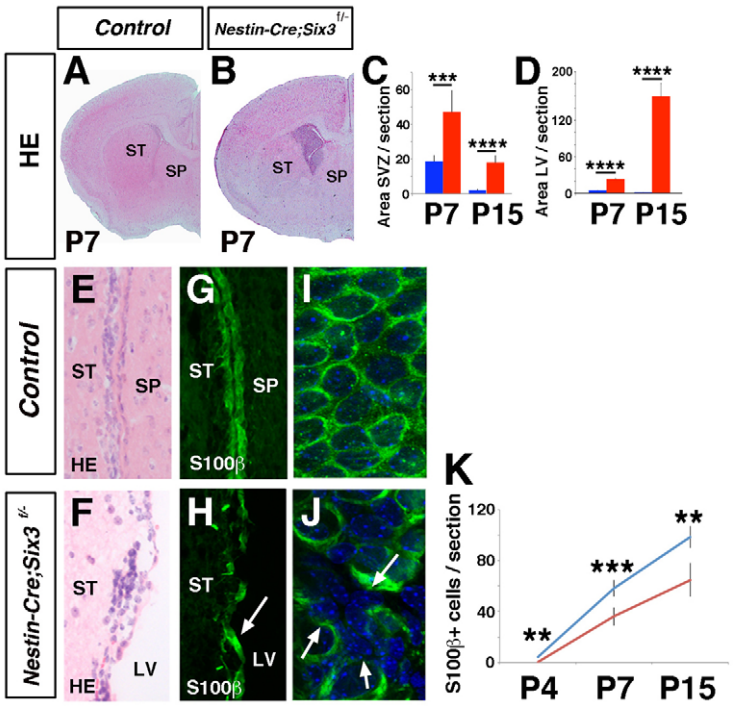

Fig. 2. Loss of Six3 at later stages of brain development results in multiple abnormalities in the neurogenic niche of the subventricular zone of the lateral ventricles. (**A**,**B**) HE staining of P7 control (A) and *Nestin-Cre;Six3*$^{f/-}$ (B) pups revealed an increase in the size of the SVZ and the LV in mutant pups. (**C**,**D**) Quantification of the area of the SVZ (C) and LV (D) in P7 and P15 control (blue) and *Nestin-Cre;Six3*$^{f/-}$ (red) pups. Data represent the mean relative area units (corrected by total area of the section) ± s.d. per section. *n*=5. (**E-J**) HE staining (E,F) and S100β IHC (G,H) of coronal sections, and whole-mount IHC of the SVZ (I,J) of control (E,G,I) and *Nestin-Cre;Six3*$^{f/-}$ (F,H,J) P15 pups showed numerous breaks in the LW of *Nestin-Cre;Six3*$^{f/-}$ pups (arrows). (**K**) The number of S100β$^+$ cells was reduced in *Nestin-Cre;Six3*$^{f/-}$ (red) mice at P4, P7 and P15. Data represent the mean number of S100β$^+$ cells per section per pup ± s.d. *n*=5 pups. ***P*<0.01, ****P*<0.001, *****P*<0.0001 determined by paired *t*-test. ST, striatum; SP, septum.

ependymal cells during the formation of the LW. We followed the temporal reduction in the number of radial glia from this region in *Nestin-Cre;Six3*$^{f/-}$ animals. Glast$^+$ cells lined the striatal side of the LV of P4 control pups (supplementary material Fig. S6A,B). At P7, some Glast$^-$ cells were also evident in the LW in wild-type pups (supplementary material Fig. S6C,D); by P15, nearly all cells in the LW of wild-type pups became Glast$^-$ (supplementary material Fig. S6E,F). However, most of the cells in the LW of *Nestin-Cre;Six3*$^{f/-}$ pups retained Glast expression from P4 to P15 (supplementary material Fig. S6G-L).

We compared the differentiation of ependymal cells in the striatal surface of the LV of control and *Nestin-Cre;Six3*$^{f/-}$ animals by analyzing vimentin expression. Few cells lining the striatal side of the LV were vimentin$^+$ in P4 wild-type pups (supplementary material Fig. S6M); at P7, some round vimentin$^+$ cells were detected (supplementary material Fig. S6N). By P15, most of the cells in the striatal side of the LV in control pups had round vimentin staining (supplementary material Fig. S6O). However, a large number of vimentin$^+$ cells with long processes similar to those of radial glia cells were present in the LW of P4 to P15 *Nestin-Cre;Six3*$^{f/-}$ littermates (supplementary material Fig. S6P-R).

To evaluate whether Six3 is necessary for the survival of ependymal cells, we performed TUNEL assays. S100β$^+$ cells were TUNEL$^-$ in both groups of mice at P4, P7 and P15 (supplementary material Fig. S7A-C). Furthermore, the number of S100β$^+$ cells increased from P4 to P15 in *Nestin-Cre;Six3*$^{f/-}$ mice (Fig. 2K). Together, these findings suggest that Six3 activity is required for the maturation of radial glia into ependymal cells.

Defective ependymal cell maturation results in cells with mixed ependymal and radial glia characteristics

Although fewer in number, some S100β$^+$ cells were present in the LW in *Nestin-Cre;Six3*$^{f/-}$ animals. The fact that the remaining S100β$^+$ cells in the P15 mice were Six3$^-$ (supplementary material Fig. S2B; Fig. 3A′,B′) brought into question whether these cells had acquired ependymal characteristics. To investigate this, we analyzed FoxJ1 expression. FoxJ1 is involved in the differentiation of ependymal cells from radial glia (Jacquet et al., 2009). Our analysis revealed fewer FoxJ1$^+$ cells in the LW at P4, P7 and P15 (supplementary material Fig. S8A-I). Furthermore, as the formation of the LW progressed, both the number of FoxJ1$^+$ cells (supplementary material Fig. S8C,F,I) and the percentage of FoxJ1$^+$ cells that were also Six3-β-Gal$^+$ (supplementary material Fig. S8J-L) increased.

Normally, ependymal cells have multiple cilia with a 9+2 ultrastructure (Bruni, 1998). Accordingly, we investigated whether the remaining cells in the mutant LW were multi-ciliated. Whole-mount S100β/acetylated tubulin (Fig. 3C,C′) or vimentin/γ-tubulin (Fig. 3D,D′) IHC of the LW in control and *Nestin-Cre;Six3*$^{f/-}$ P15 pups revealed numerous cilia on the surface of these cells. Electron microscopy showed that the cells lining the LV had cilia with a normal ultrastructure in both genotypes (Fig. 3E-H′). Although ciliogenesis seemed normal in the S100β$^+$ cells of the *Nestin-Cre;Six3*$^{f/-}$ mice, their differentiation profile could still be defective. Therefore, we analyzed whether these S100β$^+$ cells expressed noggin, a protein normally secreted by ependymal cells (Chmielnicki et al., 2004; Lim et al., 2000). We found that the S100β$^+$ cells in the LW were noggin$^+$ in both control (98.58±0.11% of the S100β$^+$ cells) and *Nestin-Cre;Six3*$^{f/-}$ (97.99±0.24%) pups at P7 (supplementary material Fig. S9A,C). It has been reported that the absence of Numb/Numbl leads to disruption of LW integrity at the LV (Kuo et al., 2006). The S100β$^+$ cells in the LW of both groups were also Numb/Numbl$^+$ (controls: 98.71±0.27% of the S100β$^+$ cells; mutant: 97.89±0.40%) (supplementary material Fig. S9B,D).

Together, all these findings suggest that the remaining S100β$^+$ cells lining the LV of *Nestin-Cre;Six3*$^{f/-}$ mice acquire normal ependymal cell features.

We investigated the possibility that the remaining S100β$^+$ cells in *Nestin-Cre;Six3*$^{f/-}$ pups could have abnormally retained radial glia characteristics during the formation of the LW. This possibility

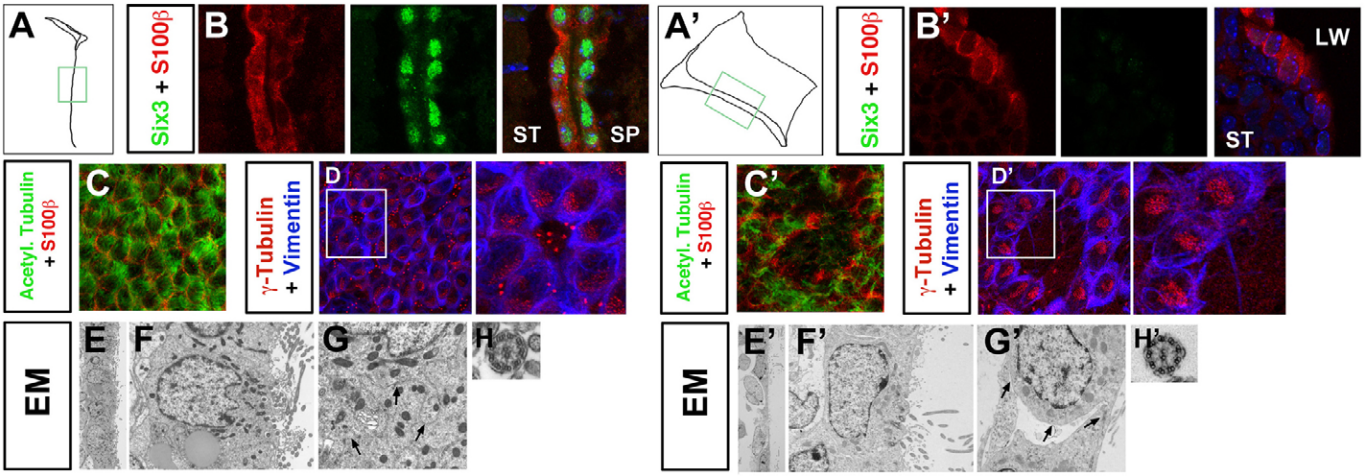

Fig. 3. Cells lining the lateral ventricles in *Nestin-Cre;Six3$^{f/-}$* mice have ependymal characteristics. (**A-B'**) IHC with an anti-Six3 antibody showed that Six3 is expressed in S100β$^+$ cells of P15 control mice (B) but not of *Nestin-Cre;Six3$^{f/-}$* mice (B′). Squares in the diagrams (A,A′) depict the dorsoventral level of the LW at which the high magnification pictures (B,B′) were taken. (**C-D'**) Acetylated tubulin/S100β (C,C′) and γ-tubulin/vimentin (D,D′) whole-mount IHC of the LW revealed the presence of multi-ciliated S100β$^+$ or vimentin$^+$ cells in P15 control (C,D) and *Six3*-conditional mutant (C′,D′) mice. (**E-H'**) Electron microscopic analysis revealed the presence of cells with ependymal cell features in contact with the LV in P15 control (E,F) and *Nestin-Cre;Six3$^{f/-}$* (E′,F′) mice. At P15, the multi-ciliated cells lining the LV were tightly linked in control animals (arrows, G), but loosely linked in *Nestin-Cre;Six3$^{f/-}$* mice (arrows, G′). Both control (H) and *Nestin-Cre;Six3$^{f/-}$* (H′) multi-ciliated cells exhibited cilia with a 9+2 structure. ST, striatum; SP, septum.

was supported by the presence of long vimentin$^+$ processes in cells lining the LV (supplementary material Fig. S6P-R) and our finding that most of the S100β$^+$ cells in the LW were also positive for Blbp (Fabp7 – Mouse Genome Informatics), a radial glia and aNSC marker (P7: 67.24±8.7%; P15: 60.78±2.5% of the S100β$^+$ cells) (Fig. 4A-D′) (Doetsch, 2003; Merkle et al., 2004), or Gfap$^+$ (P7: 92.23±6.7%; P15: 74.86±2.27% of the S100β$^+$ cells) (Fig. 4E-H′). Then, we analyzed whether the multi-ciliated cells lining the striatal side of the LV expressed a radial glia marker. Whole-mount Glast/γ-tubulin IHC revealed that, in contrast to controls, *Nestin-Cre;Six3$^{f/-}$* pups at P15 had Glast$^+$ multi-ciliated cells (supplementary material Fig. S10A,B, arrowheads). These findings showed that in the absence of Six3, the cells lining the LV have abnormally mixed ependymal and radial glia characteristics.

We also analyzed the proliferative behavior of the *Nestin-Cre;Six3$^{f/-}$* S100β$^+$ cells. Ependymal cells are postmitotic (Spassky et al., 2005) and proliferate only in response to stroke (Carlén et al., 2009). After a 1-hour BrdU pulse, no S100β$^+$BrdU$^+$ cells were found in the LW in P4, P7 and P15 control pups (Fig. 4I; supplementary material Fig. S11A-C). No S100β$^+$BrdU$^+$ cells were found in the LW in *Nestin-Cre;Six3$^{f/-}$* P4 pups (supplementary material Fig. S11D); however, they were present at P7 (3.21±0.47% of the S100β$^+$ cells) (supplementary material Fig. S11E) and P15 (2.21±0.19% of the S100β$^+$ cells) (Fig. 4J; supplementary material Fig. S11F). Similar results were observed with Ki67 (Mki67 – Mouse Genome Informatics) in the mutants at P15 (6.76±2.09% of the S100β$^+$ cells).

In the SVZ, aNSCs establish direct contact with blood vessels via long basal processes (Fig. 4K-M) (Mirzadeh et al., 2008; Shen et al., 2008). We found that S100β$^+$Gfap$^+$ cells in the LW in P15 *Nestin-Cre;Six3$^{f/-}$* mice use their long processes to contact CD31 (Pecam1 – Mouse Genome Informatics)$^+$ blood vessels (Fig. 4N-P). These findings confirm that, in the absence of Six3, the remaining S100β$^+$ cells lining the LV have both ependymal and radial glia characteristics.

Abnormal ependymal cell maturation affects neuroblast proliferation and differentiation in the SVZ

Ependymal cells are part of the SVZ neurogenic niche (Alvarez-Buylla and Lim, 2004; Doetsch, 2003); they influence proliferation and differentiation (Lim et al., 2000) and are necessary for proper neuroblast migration towards the OB during adulthood (Sawamoto et al., 2006). Therefore, we evaluated whether the abnormal ependymal cell maturation in *Nestin-Cre;Six3$^{f/-}$* pups alters cell proliferation or differentiation during the formation of the LW. We found that the number of BrdU$^+$ cells in the SVZ of *Nestin-Cre;Six3$^{f/-}$* P4 pups was similar to that of controls (Fig. 5A); however, they were more abundant at P7 (Fig. 5B) and less at P15 (Fig. 5C). A detailed double-labeling analysis was performed with BrdU and Gfap, Ascl1, Dcx and Olig2 at P4 and P7 (supplementary material Fig. S12A,B) and with Gfap, Ascl1, Dcx, Olig2 and Ng2 at P15 (supplementary material Fig. S12C). This revealed that the number of Gfap$^+$BrdU$^+$ cells was greater in the SVZ of the mutant than that of the control at P4, P7 and P15 (supplementary material Fig. S12A-C). However, the number of Ascl1$^+$BrdU$^+$ cells was also greater in the mutant at P4 and P7, but not at P15 (supplementary material Fig. S12A-C), and the number of Dcx$^+$BrdU$^+$ cells was greater in the mutant at P7 but less at P4 and P15 (supplementary material Fig. S12A-C). We found more Olig2$^+$BrdU$^+$ cells in the SVZ in *Nestin-Cre;Six3$^{f/-}$* mice at all stages (supplementary material Fig. S12A-C) and more Ng2$^+$BrdU$^+$ cells at P15 (supplementary material Fig. S12C). These findings show that there is abnormal proliferation in the SVZ in *Nestin-Cre;Six3$^{f/-}$* pups during formation of the LW.

We investigated whether the abnormal ependymal cell maturation of *Nestin-Cre;Six3$^{f/-}$* mice resulted in more cells with progenitor/stem cell properties. We quantified the primary neurospheres from cultures of the SVZ from control and *Nestin-Cre;Six3$^{f/-}$* P7 pups. We found more primary neurospheres in

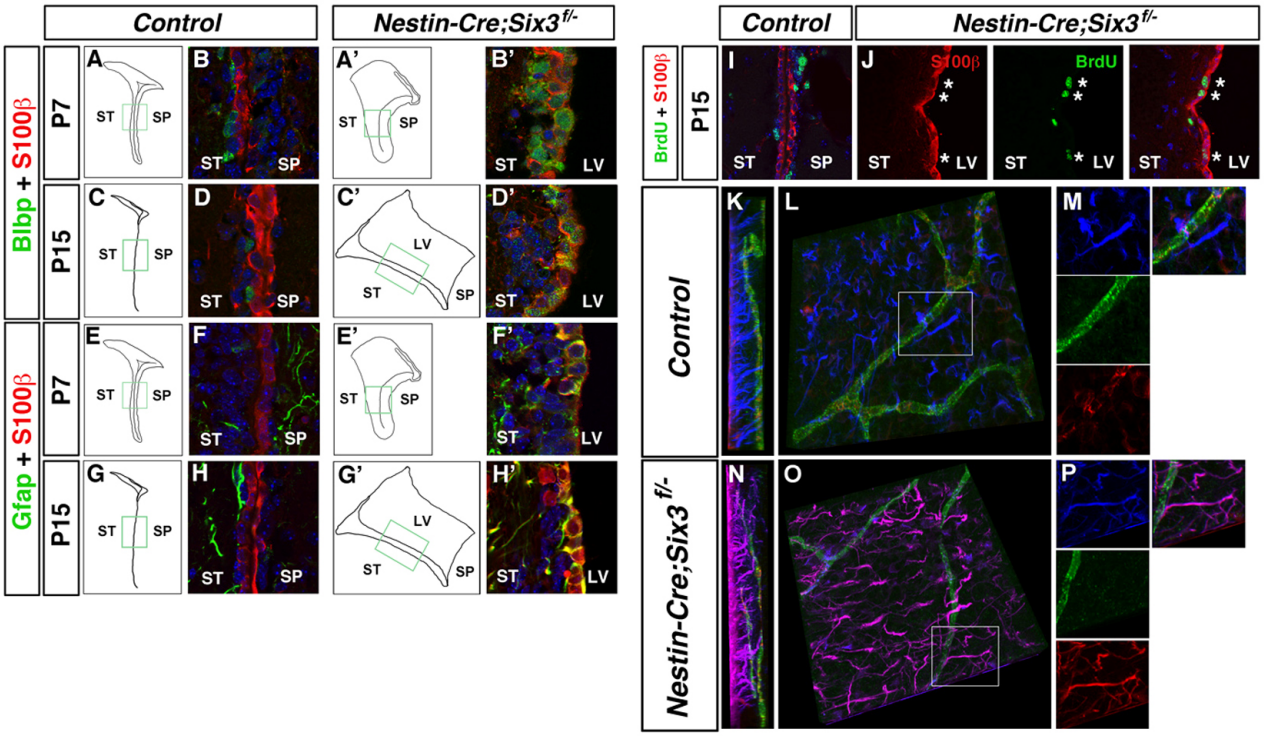

Fig. 4. S100β⁺ cells retain radial glia characteristics and interact with blood vessels in the absence of Six3. (**A-H'**) Squares in the diagrams of control (A,C,E,G) and *Nestin-Cre;Six3*$^{fl/-}$ mice (A′,C′,E′,G′) depict the dorsoventral level of the LW at which the high magnification pictures of P7 and P15 control and *Nestin-Cre;Six3*$^{fl/-}$ were taken. S100β⁺ cells were Blbp⁻ (B,D) and Gfap⁻ (F,H) in P7 (B,F) and P15 (D,H) control pups. However, in P7 *Nestin-Cre;Six3*$^{fl/-}$ pups, most S100β⁺ cells were Blbp⁺ (B′) or Gfap⁺ (F′). Many S100β⁺ cells in P15 *Six3* conditional mutant pups were also Blbp⁺ (D′) and Gfap⁺ (H′). (**I**,**J**) At P15, S100β⁺ cells of control mice were not proliferating, as indicated by BrdU staining (I); however, a few S100β⁺BrdU⁺ (asterisks, J) cells were detected in *Nestin-Cre;Six3*$^{fl/-}$ mice. (**K**) Lateral view of whole-mount Gfap/S100β/CD31 IHC of the SVZ (left, surface of the LW) shows that Gfap⁺ (blue) cells but not S100β⁺ (red) cells projected long processes towards the CD31⁺ (green) blood vessels in P15 control mice. (**L**) 90-degree rotation view of the Gfap/S100β/CD31 whole-mount IHC shown in K revealing the interaction of a Gfap⁺ cell with a CD31⁺ blood vessel (inset). (**M**) High magnification panels of the inset in L. (**N**) Lateral view of whole-mount Gfap/S100β/CD31 IHC of the SVZ (left, surface of the LW) shows that Gfap⁺S100β⁺ cells projected long processes towards the CD31⁺ (green) blood vessels in P15 *Nestin-Cre;Six3*$^{fl/-}$ mice. (**O**) 90-degree rotation view of the Gfap/S100β/CD31 whole-mount IHC shown in N revealing the interaction of a Gfap⁺S100β⁺ cell with a CD31⁺ blood vessel (inset). (**P**) High magnification panels of the inset in O. ST, striatum; SP, septum.

cultures from *Nestin-Cre;Six3*$^{fl/-}$ pups, suggesting the presence of more cells with progenitor/stem cell potential (supplementary material Fig. S13A).

We investigated whether defective LW formation and abnormal proliferation affected SVZ neurogenesis in *Nestin-Cre;Six3*$^{fl/-}$ mice. We found that the number of Gfap⁺ astrocytes was lower in the SVZ of mutants than controls at P4 (Fig. 5G; supplementary material Fig. S14A) and greater at P7 and P15 (Fig. 5H,I; supplementary material Fig. S14B,C). The number of Ascl1⁺ cells was higher in mutants at P4 and P7 (Fig. 5J,K; supplementary material Fig. S14A,B) and was similar in mutants and controls at P15 (Fig. 5L; supplementary material Fig. S14C). The number of Olig2⁺ (Fig. 5M-O; supplementary material Fig. S14A-C) and Dcx⁺ (Fig. 5P-R; supplementary material Fig. S14A-C) cells was higher in mutants at all stages analyzed. The number of Ng2⁺ cells was greater in mutants at P15 (Fig. 5S; supplementary material Fig. S14C). These findings, together with the increase in the number of Gfap⁺BrdU⁺, Olig2⁺BrdU⁺ and Ng2⁺BrdU⁺ cells, suggest that glial differentiation is augmented in the SVZ in *Nestin-Cre;Six3*$^{fl/-}$ pups. However, the number of β-Tub-III⁺, Gfap⁺ and Ng2⁺ cells in control and *Nestin-Cre;Six3*$^{fl/-}$ neurospheres was the same (supplementary material Fig. S13B-G). These findings suggest that the increase in the number glial cells in *Nestin-Cre;Six3*$^{fl/-}$ mice is a non-cell autonomous consequence of the abnormal ependymal cell maturation and of LW damage.

We then evaluated whether *Six3* mutant cells could contribute to the size increase observed in the mutant SVZ. We followed the fate of the 'should-be' Six3-expressing cells using the β-gal allele inserted into the *Six3* locus. At P7, the SVZ of control pups contained only Six3-β-Gal⁺ cells lining the LV; however, there were Six3-β-Gal⁺ cells inside the SVZ of *Nestin-Cre;Six3*$^{fl/-}$ pups (201.95±50 Six3-β-Gal⁺ cells/section, 4.96±1.34% of DAPI⁺ cells inside the SVZ). Next, we characterized these Six3-β-Gal⁺ cells by performing double IHC with Six3-β-Gal⁺ and Gfap (supplementary material Fig. S15A-D), Ascl1 (supplementary material Fig. S15E-H), Olig2 (supplementary material Fig. S15I-L) or Dcx (supplementary material Fig. 15M-P). Only Six3-β-Gal⁺Dcx⁺ cells were detected following this analysis (141.62±23.08 Six3-β-Gal⁺Dcx⁺ cells/section) (supplementary material Fig. S15M-P); most of the Six3-β-Gal⁺ were Dcx⁺ (71.82±12.80% of the Six3-β-Gal⁺ cells were Dcx⁺), but only a small percentage of the Dcx⁺ cells in the SVZ in *Nestin-Cre;Six3*$^{fl/-}$ pups were also Six3-β-Gal⁺ (3.52±0.54% of

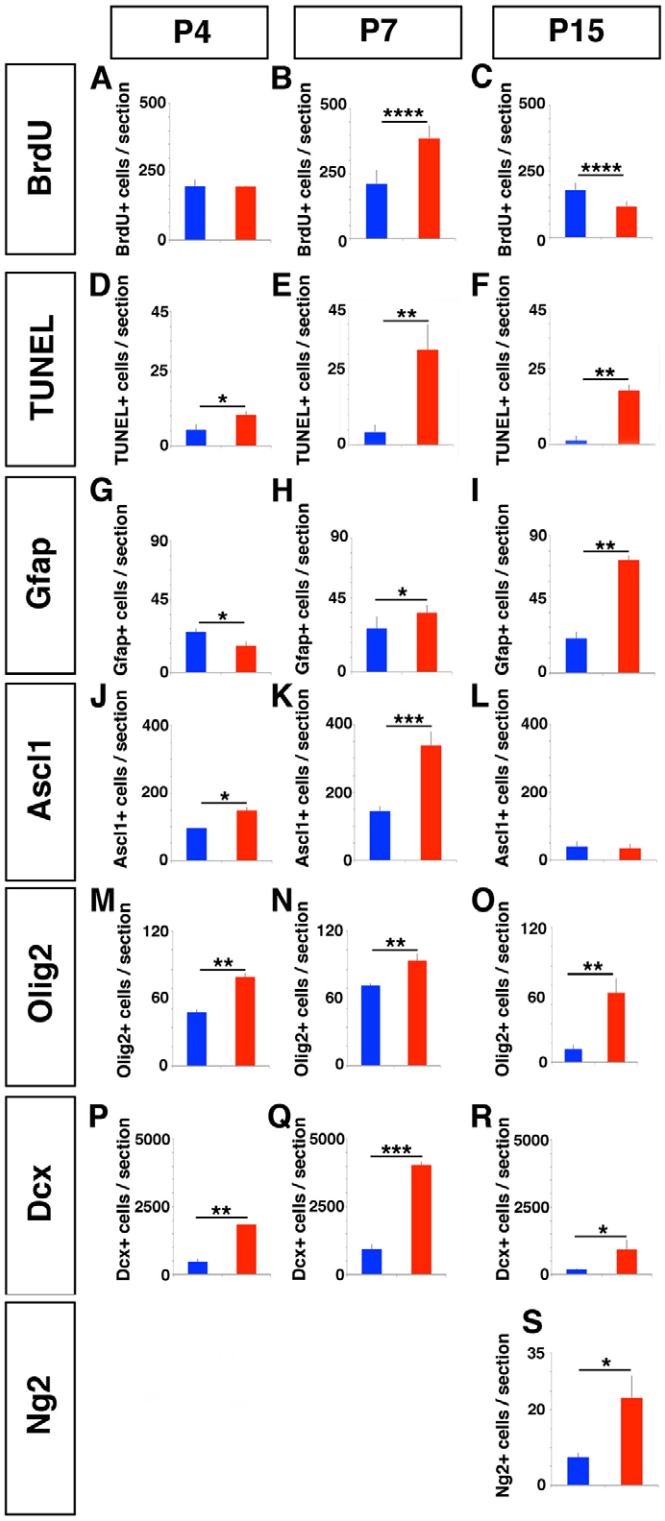

Fig. 5. Defective ependymal cell maturation leads to abnormal proliferation and differentiation in the SVZ of *Nestin-Cre;Six3$^{f/-}$* mice. (**A-S**) The number of BrdU$^+$ cells in the SVZ of the mutant pups (red bars) was similar to that of control littermates (blue bars) at P4 (A), greater at P7 (B) and smaller at P15 (C). The number of TUNEL$^+$ cells in the SVZ of *Nestin-Cre;Six3$^{f/-}$* pups was greater than that of control littermates at P4 (D), P7 (E) and P15 (F). The number of Gfap$^+$ cells in the SVZ in *Nestin-Cre;Six3$^{f/-}$* pups was smaller at P4 (G) but greater at P7 (H) and P15 (I) than in control pups. The number of Ascl1$^+$ cells in the SVZ in *Nestin-Cre;Six3$^{f/-}$* pups was greater than in control littermates at P4 (J) and P7 (K) but similar at P15 (L). The number of Olig2$^+$ cells was greater in the SVZ of the LV in *Nestin-Cre;Six3$^{f/-}$* mice at P4 (M), P7 (N) and P15 (O). The number of Dcx$^+$ cells in the SVZ of the LV was increased in *Nestin-Cre;Six3$^{f/-}$* mice at P4 (P), P7 (Q) and P15 (R). The number of Ng2$^+$ cells was greater in the SVZ of the LV in P15 *Nestin-Cre;Six3$^{f/-}$* pups (S). Data represent the mean of the number of positive cells per section per pup ± s.d. n=5 pups in A-F, n=3 pups in G-O,V. *P<0.1, **P<0.01, ***P<0.001, ****P<0.0001 determined by paired t-test.

DAPI$^+$ cells were also Six3-β-Gal$^+$Dcx$^+$). These findings showed that *Six3* mutant cells have a small contribution to the increase in size of the SVZ in P7 *Nestin-Cre;Six3$^{f/-}$* pups.

We compared the size of the rostral migratory stream (RMS) in P7 control and *Nestin-Cre;Six3$^{f/-}$* pups. P0-induced ependymal wall defects and increased neuroblast apoptosis reduces the size of the OB and the RMS (Kuo et al., 2006). Furthermore, ependymal cell function is required for proper neuroblast migration to the OB in adult animals (Sawamoto et al., 2006). We found that, although Six3 is not expressed in the RMS or the OB (supplementary material Fig. S16A,B), the RMS in P7 *Nestin-Cre;Six3$^{f/-}$* pups was smaller than that of control littermates (supplementary material Fig. S16C). This suggests that the enlarged SVZ in *Nestin-Cre;Six3$^{f/-}$* mice is due to increased proliferation and possibly also to defective neuroblast migration.

Postnatal deletion of Six3 affects ependymal cell maturation

To determine whether the enlarged LV could be a result of Six3 function in the ventricular system, we analyzed its expression pattern in the choroid plexus (CP) and subcommissural organ (SCO) in E12.5, P4 and P15 control mice. We found Six3 expression in the CP at E12.5 but not at P4 or P15, and not in the SCO at any of the stages analyzed (supplementary material Fig. S17A,B). Furthermore, we did not observe any obvious morphological abnormalities in the CP at P0 (supplementary material Fig. S17C,D), the SCO at P15 (supplementary material Fig. S17 E-J) or the Sylvian aqueduct at P15 (supplementary material Fig. S17K,L). To narrow the time frame during which Six3 activity is required in the SVZ, and to avoid any possible functional consequence of Six3 loss in the CP at E12.5, we took advantage of a tamoxifen-inducible *Nestin-CreER^{T2}* strain (Cicero et al., 2009). Tamoxifen induction from P0 to P5 was sufficient to remove Six3 from about 50% of the vimentin$^+$ cells in the LW (supplementary material Fig. S2C) and enlarge the SVZ (Fig. 6A-B) and the LV (Fig. 6A,A′,B′) of P15 *Nestin-CreER^{T2};Six3$^{f/-}$* brains. Furthermore, S100β staining revealed that the LW was discontinuous (Fig. 6C-D′) and had fewer S100β$^+$ cells, some of which co-expressed Gfap (Fig. 6E-F′) or exhibited long processes (Fig. 6D′,F′). Whole-mount-vimentin/γ-tubulin IHC showed that vimentin$^+$ cells lining the LW were multi-ciliated in P15 controls (Fig. 6G) and *Nestin-CreER^{T2};Six3$^{f/-}$* littermates (Fig. 6G′). Furthermore, whole-mount Glast/γ-tubulin IHC showed that in P15 control pups, all the multi-ciliated cells were Glast$^-$ (Fig. 6H), but in *Nestin-CreER^{T2};Six3$^{f/-}$* littermates, some of the multi-ciliated cells were found to be Glast$^+$ (Fig. 6H′). A small percentage of the *Nestin-*

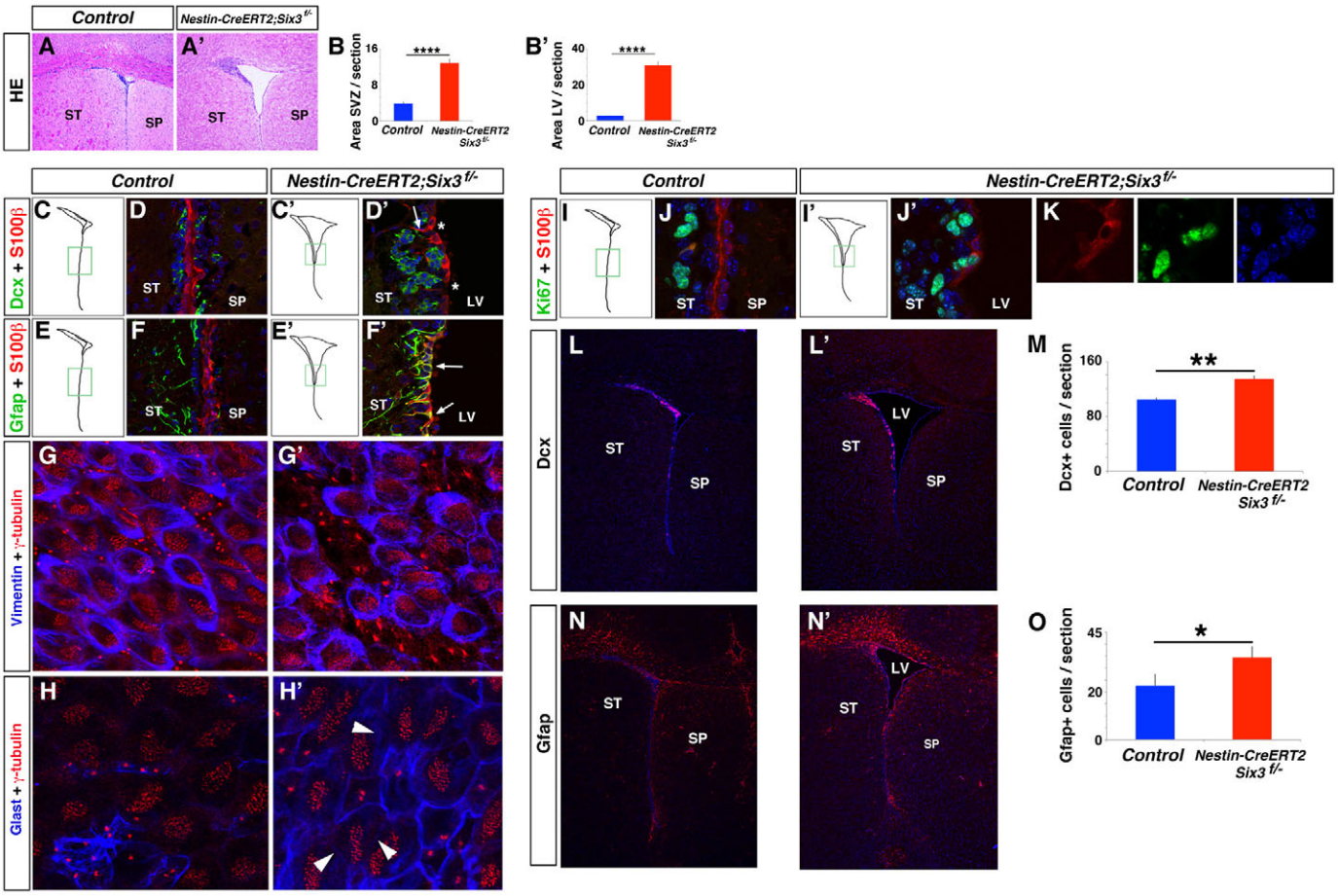

Fig. 6. Postnatal deletion of *Six3* results in abnormal ependymal cell maturation. (**A-B'**) HE staining of coronal sections of control (A) and *Nestin-CreERT2;Six3*$^{f/-}$ (A') brains revealed an increase in the size of the dorsal SVZ and LV in *Nestin-CreERT2;Six3*$^{f/-}$ brain. This size increase is also shown in the graphs for the SVZ (B) and the LV (B') of P15 control (blue) and *Nestin-CreERT2;Six3*$^{f/-}$ (red) mice. Data in B and B' represent the mean relative area units (corrected by total area of the section) per section per pup ± s.d. *n*=3 pups. (**C-F',I-K**) Squares in the diagrams (C,C',E,E',I,I') depict the dorsoventral level of the LW of the LV at which the high magnification pictures (D,D',F,F',J,J') were taken. S100β staining at P15 showed that the LW of control pups is continuous (D,F); however, that of *Nestin-CreERT2;Six3*$^{f/-}$ mice had breaks (asterisks, D'). The P15 *Nestin-CreERT2;Six3*$^{f/-}$ mice also had fewer S100β$^+$ cells (61.27±6.29 cells per LW section per pup) than the controls (87.1±9.96 cells per LW section per pup) (*n*=3 pups; *P*<0.0001). Moreover, S100β$^+$ cells in the LW of the LV of P15 *Nestin-CreERT2;Six3*$^{f/-}$ pups had processes (arrow, D') and were Gfap$^+$ (F') whereas those of controls did not (D,F). A small portion of S100β$^+$ cells in the SVZ of P15 *Nestin-CreERT2;Six3*$^{f/-}$ were also Ki67$^+$ (J' and higher magnification in K); no S100β$^+$/Ki67$^+$ cells were present in controls (J). (**G-H'**) Vimentin/γ-tubulin whole-mount IHC of the LW showed that vimentin$^+$ cells in both control (G) and *Six3* conditional mutant (G') P15 pups have multiple cilia. Glast/γ-tubulin whole-mount IHC of the LW showed that in control P15 pups only single-ciliated cells are Glast$^+$ (H). However, some multi-ciliated cells were Glast$^+$ in *Nestin-CreERT2;Six3*$^{f/-}$ P15 pups (arrowheads, H'). (**L-O**) There were more Dcx$^+$ (L',M) and Gfap$^+$ (N',O) cells in the SVZ in P15 *Nestin-CreERT2;Six3*$^{f/-}$ mice than in the controls (L-O). Data in M and O represent the number of Dcx$^+$ (M) and Gfap$^+$ (O) cells in control (blue) and *Six3*-conditional mutant mice (red) per section per pup. *n*=3 pups. *P<0.1, **P<0.01, ****P<0.0001 determined by paired *t*-test. ST, striatum; SP, septum.

CreER^{T2}*;Six3*$^{f/-}$ S100β$^+$ cells were Ki67$^+$, indicating that they proliferate (2.76±0.53% of the S100β$^+$ cells) (Fig. 6I-K). The SVZ in mutant mice also had more Dcx$^+$ (Fig. 6L-M) and Gfap$^+$ (Fig. 6N-O) cells.

Together, these findings show that postnatal deletion of Six3 is sufficient to affect ependymal maturation and that the abnormal differentiation of cells in the SVZ is due to abnormal ependymal cell maturation.

DISCUSSION

Six3 is normally expressed in the Gfap$^-$Ascl1$^-$Dcx$^-$Olig2$^-$Ng2$^-$Glast$^-$FoxJ1$^+$vimentin$^+$S100β$^+$ population of the LW postnatally, and its expression pattern follows the normal temporal and spatial pattern of ependymal cell maturation. As the transformation of ependymal cells progresses and more FoxJ1$^+$ cells acquire ependymal characteristics, the number of Six3-β-Gal$^+$FoxJ1$^+$ cells in the LW increases, and nearly all the S100β$^+$ cells lining the LV express Six3. Inactivation of Six3 in *Nestin-Cre;Six3*$^{f/-}$ or *Nestin-CreERT2*^{T2}*;Six3*$^{f/-}$ mice leads to S100β$^+$ cells with mixed ependymal/radial glia characteristics. This suggests that during ependymal cell differentiation, Six3 is required to suppress radial glia properties but not for the acquisition of ependymal characteristics. This could be the first example of a differentiation defect in ependymal cell formation that does not block the acquisition of ependymal cell properties but does block the disappearance of a radial glia fate. S100β$^+$ cells in *Six3* conditional

mutant mice acquire ependymal characteristics; accordingly FoxJ1, a protein necessary for acquiring ependymal properties (Jacquet et al., 2009; Paez-Gonzalez et al., 2011), is expressed in nearly all Six3-β-Gal$^+$ cells in the LW at P15.

Our findings also show that Six3 inactivation leads to a reduction in the number of FoxJ1$^+$ and S100β$^+$ cells. This reduction suggests that Six3 could also be required in radial glia at the embryonic stages when the ependymal cells are born; however, Six3 is not expressed in radial glia in the basal telencephalon at E12.5 or later (supplementary material Fig. S5). Furthermore, Six3 is not required for ependymal cell survival, as no S100β$^+$TUNEL$^+$ cells were observed in the SVZ in *Nestin-Cre;Six3$^{f/-}$* mice at any of the analyzed stages. Another possible explanation for the reduction in the number of S100β$^+$ cells in the *Six3*-conditional mutant mice could be the generation of FoxJ1$^-$ cells that do not express S100β or have motile ciliogenesis (Jacquet et al., 2009; Paez-Gonzalez et al., 2011). However, Six3 seems to be temporally downstream of FoxJ1, as FoxJ1 expression is detected in the ventricular zone (VZ) as early as E14 (Jacquet et al., 2009); instead, as previously mentioned, Six3 expression was not observed in the VZ of the basal telencephalon at E12.5, E14.5, E16.5 or P0 (supplementary material Fig. S5). Furthermore, as the formation of the LW progresses during development, the number of FoxJ1$^+$Six3-β-Gal$^+$ cells increases (supplementary material Fig. S8). Because FoxJ1 is necessary for both the loss of radial glia properties and the acquisition of ependymal characteristics, our findings raise the question of whether FoxJ1 regulates Six3 expression during ependymal cell maturation or whether FoxJ1 and Six3 cooperate in the loss of radial glia properties. However, Six3 is co-expressed with FoxJ1 only in ependymal cells, as Six3 is not expressed in astrocytes or in the OB; this difference in expression pattern between Six3 and FoxJ1 explains the differences between our findings and those of Jacquet et al. (Jacquet et al., 2011). Furthermore, as FoxJ1 is expressed in S100β$^+$ cells during and after the formation of the LW, it is possible that the loss of S100β$^+$ is the main reason for the reduction in the number of FoxJ1$^+$ cells in *Nestin-Cre;Six3$^{f/-}$* mice. One possible explanation for this loss of S100β$^+$ cells could be a denudation of the mixed ependymal/radial glia cells from the LW of *Nestin-Cre;Six3$^{f/-}$* mice due to their cell adhesion defects, as revealed by the lack of F-actin apical border expression in the LW. Another possible explanation could be the differentiation of some of the mixed ependymal/radial glia cells into neurons or glia cells. This has been previously described in response to stroke, when the number of ependymal cells is reduced because they give rise to neuroblasts and astrocytes (Carlén et al., 2009). Accordingly, we observed double Dcx$^+$Six3-β-Gal$^+$ cells in the SVZ of P7 *Nestin-Cre;Six3$^{f/-}$* pups. However, it seems unlikely that these cells originate from cells with mixed ependymal/radial glia characteristics because in the SVZ of the *Nestin-Cre;Six3$^{f/-}$* mice we did not find cells with intermediate progenitor characteristics (Ascl1$^+$Six3-β-Gal$^+$). Furthermore, as all of the remaining S100β$^+$ cells in *Nestin-Cre;Six3$^{f/-}$* mice were Six3$^-$, we cannot currently explain why some mutant cells remained or why others presumably differentiated towards a neuronal fate.

We also showed that one consequence of defective ependymal cell maturation in *Nestin-Cre;Six3$^{f/-}$* and *Nestin-CreERT2;Six3$^{f/-}$* mice is the presence of breaks along the LW. This aberration was probably due to the reduced number of ependymal cells or the defects in cell adhesion observed in the LW. The absence of an enlarged LV at P0 and the recapitulation of the LV and LW phenotypes in *Nestin-CreERT2;Six3$^{f/-}$* mice in the absence of Six3 expression in the CP suggests that the hydrocephaly observed in *Six3*-conditional mutant pups is an indirect consequence of the damage in the LW. A similar phenotype has been described for *Numb/Numbl* conditional mutant mice (Kuo et al., 2006). In those animals, the LW contains numerous breaks resulting from the lack of cell adhesion molecules such as F-actin and E-cadherin (Kuo et al., 2006). Although we found a similar deficit in the expression of F-actin in the LW of *Nestin-Cre;Six3$^{f/-}$* pups, we did not find reduced levels of *Numb/Numbl*, indicating that Six3 does not control *Numb/Numbl* expression.

Under normal conditions, S100β$^+$ ependymal cells are quiescent (Spassky et al., 2005); however, in response to a stroke, they lose ependymal features, proliferate and generate new neuroblasts and astrocytes (Carlén et al., 2009). However, we found proliferating S100β$^+$ cells scattered along the LW in *Nestin-Cre;Six3$^{f/-}$* mice. Therefore, it is possible that proliferating S100β$^+$ cells generate other S100β$^+$ cells in *Six3*-conditional mutant mice. Interestingly, in 6-week-old *Numb/Numbl* conditional mutant mice, the damaged LW is eventually repaired by Gfap$^+$S100β$^+$ cells and Glast$^+$ cells (Kuo et al., 2006). These cells are not normally present in the SVZ and, based on their expression profile, they appear to correspond to the hybrid ependymal/radial glia cells that we found in the *Six3* conditional mutant brain. Unfortunately, owing to the early postnatal death of *Six3* conditional mutant mice (most likely due to severe pituitary alterations; data not shown), we were not able to evaluate whether the ependymal/radial glia cells can eventually also repair the damaged LW by generating more hybrid ependymal/radial glia cells.

The increase in size of the SVZ seems to be a non-cell autonomous consequence of abnormal ependymal cell maturation and increased proliferation, as Six3 is not expressed in astrocytes or progenitors in the SVZ at the stages analyzed. However, it is also possible that, as ventral SVZ neurogenesis could be regulated by forebrain neurons (Ihrie et al., 2011), part of the increase in the size of the SVZ in the *Six3* conditional mutant mice could be due to a non-cell autonomous effect of the lack of Six3 in other brain areas. Either the increased pressure due to the hydrocephaly or the increased number of cells in the SVZ could cause the increase in cell death observed in this region. The differentiation of astrocytes and oligodendrocytes was higher in *Six3*-conditional mutants than in controls; this could have been caused by a reduction in either the level of noggin as a consequence of the reduction in the number of ependymal cells or by increased pressure in the LV.

In summary, we have provided evidence that Six3 plays a role in the loss of radial glia characteristics during postnatal ependymal cell maturation. In the absence of Six3, the LW is damaged; this results in abnormal neuroblast proliferation, differentiation and migration and, ultimately, hydrocephaly.

Acknowledgements

We thank Suzanne Baker and Guo Zhu for the *Nestin-CreER^{T2}* mouse line and for sharing *Nestin-CreER^{T2};R26R* and *Nestin-CreER^{T2};R26YFP* reagents. We thank Young-Goo Han and Xin Gen for critical reading of this manuscript and for helpful discussion and suggestions. We also thank David Galloway for the editing of this manuscript.

Funding

This work was supported in part by the National Institutes of Health [EYEY12162 to G.O.]; Cancer Center Support [CA-21765]; and the American Lebanese Syrian Associated Charities (ALSAC). Deposited in PMC for release after 12 months.

Competing interests statement

The authors declare no competing financial interests.

Supplementary material

Supplementary material available online at
http://dev.biologists.org/lookup/suppl/doi:10.1242/dev.067470/-/DC1

References

Alvarez-Buylla, A. and Garcia-Verdugo, J. M. (2002). Neurogenesis in adult subventricular zone. *J. Neurosci.* **22**, 629-634.

Alvarez-Buylla, A. and Lim, D. A. (2004). For the long run: maintaining germinal niches in the adult brain. *Neuron* **41**, 683-686.

Betz, U. A., Vosshenrich, C. A., Rajewsky, K. and Muller, W. (1996). Bypass of lethality with mosaic mice generated by Cre-loxP-mediated recombination. *Curr. Biol.* **6**, 1307-1316.

Bruni, J. E. (1998). Ependymal development, proliferation, and functions: a review. *Microsc. Res. Tech.* **41**, 2-13.

Carlén, M., Meletis, K., Göritz, C., Darsalia, V., Evergren, E., Tanigaki, K., Amendola, M., Barnabé-Heider, F., Yeung, M. S. Y., Naldini, L. et al. (2009). Forebrain ependymal cells are Notch-dependent and generate neuroblasts and astrocytes after stroke. *Nat. Neurosci.* **12**, 259-267.

Chmielnicki, E., Benraiss, A., Economides, A. N. and Goldman, S. A. (2004). Adenovirally expressed noggin and brain-derived neurotrophic factor cooperate to induce new medium spiny neurons from resident progenitor cells in the adult striatal ventricular zone. *J. Neurosci.* **24**, 2133-2142.

Cicero, S. A., Johnson, D., Reyntjens, S., Frase, S., Connell, S., Chow, L. M., Baker, S. J., Sorrentino, B. P. and Dyer, M. A. (2009). Cells previously identified as retinal stem cells are pigmented ciliary epithelial cells. *Proc. Natl. Acad. Sci. USA* **106**, 6685-6690.

Conte, I., Morcillo, J. and Bovolenta, P. (2005). Comparative analysis of Six 3 and Six 6 distribution in the developing and adult mouse brain. *Dev. Dyn.* **234**, 718-725.

Didier, M., Harandi, M., Aguera, M., Bancel, B., Tardy, M., Fages, C., Calas, A., Stagaard, M., Mollgard, K. and Belin, M. F. (1986). Differential immunocytochemical staining for glial fibrillary acidic (GFA) protein, S-100 protein and glutamine synthetase in the rat subcommissural organ, nonspecialized ventricular ependyma and adjacent neuropil. *Cell Tissue Res.* **245**, 343-351.

Doetsch, F. (2003). A niche for adult neural stem cells. *Curr. Opin. Genet. Dev.* **13**, 543-550.

Doetsch, F. and Alvarez-Buylla, A. (1996). Network of tangential pathways for neuronal migration in adult mammalian brain. *Proc. Natl. Acad. Sci. USA* **93**, 14895-14900.

Doetsch, F., García-Verdugo, J. M. and Alvarez-Buylla, A. (1997). Cellular composition and three-dimensional organization of the subventricular germinal zone in the adult mammalian brain. *J. Neurosci.* **17**, 5046-5061.

Geng, X., Speirs, C., Lagutin, O., Inbal, A., Liu, W., Solnica-Krezel, L., Jeong, Y., Epstein, D. J. and Oliver, G. (2008). Haploinsufficiency of Six3 fails to activate Sonic hedgehog expression in the ventral forebrain and causes holoprosencephaly. *Dev. Cell* **15**, 236-247.

Ihrie, R. A., Shah, J. K., Harwell, C. C., Levine, J. H., Guinto, C. D., Lezameta, M., Kriegstein, A. R. and Alvarez-Buylla, A. (2011). Persistent sonic hedgehog signaling in adult brain determines neural stem cell positional identity. *Neuron* **71**, 250-262.

Jacquet, B. V., Salinas-Mondragon, R., Liang, H., Therit, B., Buie, J. D., Dykstra, M., Campbell, K., Ostrowski, L. E., Brody, S. L. and Ghashghaei, H. T. (2009). FoxJ1-dependent gene expression is required for differentiation of radial glia into ependymal cells and a subset of astrocytes in the postnatal brain. *Development* **136**, 4021-4031.

Jacquet, B. V., Muthusamy, N, Sommerville, L. J., Xiao, G., Liang, H., Zhang, Y., Holtzman and M. J., Ghashghaei, H. T. (2011). Specification of a Foxj1-dependent lineage in the forebrain is required for embryonic-to-postnatal transition of neurogenesis in the olfactory bulb. *J. Neurosci.* **31**, 9368-9382.

Kuo, C. T., Mirzadeh, Z., Soriano-Navarro, M., Rasin, M., Wang, D., Shen, J., Sestan, N., Garcia-Verdugo, J., Alvarez-Buylla, A., Jan, L. Y. et al. (2006). Postnatal deletion of Numb/Numblike reveals repair and remodeling capacity in the subventricular neurogenic niche. *Cell* **127**, 1253-1264.

Lagutin, O. V., Zhu, C. C., Kobayashi, D., Topczewski, J., Shimamura, K., Puelles, L., Russell, H. R., McKinnon, P. J., Solnica-Krezel, L. and Oliver, G. (2003). Six3 repression of Wnt signaling in the anterior neuroectoderm is essential for vertebrate forebrain development. *Genes Dev.* **17**, 368-379.

Lavado, A. and Oliver, G. (2007). Prox1 expression patterns in the developing and adult murine brain. *Dev. Dyn.* **236**, 518-524.

Lavado, A., Lagutin, O. V. and Oliver, G. (2008). Six3 inactivation causes progressive caudalization and aberrant patterning of the mammalian diencephalon. *Development* **135**, 441-450.

Lim, D. A., Tramontin, A. D., Trevejo, J. M., Herrera, D. G., García-Verdugo, J. M. and Alvarez-Buylla, A. (2000). Noggin antagonizes BMP signaling to create a niche for adult neurogenesis. *Neuron* **28**, 713-726.

Liu, W., Lagutin, O. V., Mende, M., Streit, A. and Oliver, G. (2006). Six3 activation of Pax6 expression is essential for mammalian lens induction and specification. *EMBO J.* **25**, 5383-5395.

Liu, W., Lagutin, O., Swindell, E., Jamrich, M. and Oliver, G. (2010). Neuroretina specification in mouse embryos requires Six3-mediated suppression of Wnt8b in the anterior neural plate. *J. Clin. Invest.* **120**, 3568-3577.

Lois, C. and Alvarez-Buylla, A. (1994). Long-distance neuronal migration in the adult mammalian brain. *Science* **264**, 1145-1148.

Merkle, F. T., Tramontin, A. D., García-Verdugo, J. M. and Alvarez-Buylla, A. (2004). Radial glia give rise to adult neural stem cells in the subventricular zone. *Proc. Natl. Acad. Sci. USA* **101**, 17528-17532.

Miller, F. D. and Gauthier-Fisher, A. E. (2009). Home at last: neural stem cell niches defined. *Cell Stem Cell* **4**, 507-510.

Mirzadeh, Z., Merkle, F., Sorianonavarro, M., Garciaverdugo, J. and Alvarezbuylla, A. (2008). Neural stem cells confer unique pinwheel architecture to the ventricular surface in neurogenic regions of the adult brain. *Cell Stem Cell* **3**, 265-278.

Oliver, G., Mailhos, A., Wehr, R., Copeland, N. G., Jenkins, N. A. and Gruss, P. (1995). Six3, a murine homologue of the sine oculis gene, demarcates the most anterior border of the developing neural plate and is expressed during eye development. *Development* **121**, 4045-4055.

Paez-Gonzalez, P., Abdi, K., Luciano, D., Liu, Y., Soriano-Navarro, M., Rawlins, E., Bennett, V., Garcia-Verdugo, J. M., Kuo, C. T. (2011) Ank3-dependent SVZ niche assembly is required for the continued production of new neurons. *Neuron* **71**, 61-75.

Porter, F. D., Drago, J., Xu, Y., Cheema, S. S., Wassif, C., Huang, S. P., Lee, E., Grinberg, A., Massalas, J. S., Bodine, D. et al. (1997). Lhx2, a LIM homeobox gene, is required for eye, forebrain, and definitive erythrocyte development. *Development* **124**, 2935-2944.

Porteus, M. H., Bulfone, A., Ciaranello, R. D. and Rubenstein, J. L. (1991). Isolation and characterization of a novel cDNA clone encoding a homeodomain that is developmentally regulated in the ventral forebrain. *Neuron* **7**, 221-229.

Ramírez-Castillejo, C., Sánchez-Sánchez, F., Andreu-Agulló, C., Ferrón, S. R., Aroca-Aguilar, J. D., Sánchez, P., Mira, H., Escribano, J. and Fariñas, I. (2006). Pigment epithelium-derived factor is a niche signal for neural stem cell renewal. *Nat. Neurosci.* **9**, 331-339.

Reynolds, B. A. and Weiss, S. (1992). Generation of neurons and astrocytes from isolated cells of the adult mammalian central nervous system. *Science* **255**, 1707-1710.

Sawamoto, K., Wichterle, H., Gonzalez-Perez, O., Cholfin, J. A., Yamada, M., Spassky, N., Murcia, N. S., Garcia-Verdugo, J. M., Marin, O., Rubenstein, J. L. et al. (2006). New neurons follow the flow of cerebrospinal fluid in the adult brain. *Science* **311**, 629-632.

Schaeren-Wiemers, N. and Gerfin-Moser, A. (1993). A single protocol to detect transcripts of various types and expression levels in neural tissue and cultured cells: in situ hybridization using digoxigenin-labelled cRNA probes. *Histochemistry* **100**, 431-440.

Schnitzer, J., Franke, W. W. and Schachner, M. (1981). Immunocytochemical demonstration of vimentin in astrocytes and ependymal cells of developing and adult mouse nervous system. *J. Cell. Biol.* **90**, 435-447.

Shen, Q., Wang, Y., Kokovay, E., Lin, G., Chuang, S., Goderie, S., Roysam, B. and Temple, S. (2008). Adult SVZ stem ells lie in a vascular niche: a quantitative analysis of niche cell-cell interactions. *Cell Stem Cell* **3**, 289-300.

Shibata, T., Yamada, K., Watanabe, M., Ikenaka, K., Wada, K., Tanaka, K. and Inoue, Y. (1997). Glutamate transporter GLAST is expressed in the radial glia-astrocyte lineage of developing mouse spinal cord. *J. Neurosci.* **17**, 9212-9219.

Spassky, N., Merkle, F. T., Flames, N., Tramontin, A. D., García-Verdugo, J. M. and Alvarez-Buylla, A. (2005). Adult ependymal cells are postmitotic and are derived from radial glia cells during embryogenesis. *J. Neurosci.* **25**, 10-18.

Tavazoie, M., Vanderveken, L., Silvavargas, V., Louissaint, M., Colonna, L., Zaidi, B., Garciaverdugo, J. and Doetsch, F. (2008). A specialized vascular niche for adult neural stem cells. *Cell Stem Cell* **3**, 279-288.

Yu, X., Ng, C. P., Habacher, H. and Roy, S. (2008). Foxj1 transcription factors are master regulators of the motile ciliogenic program. *Nat. Genet.* **40**, 1445-1453.

Zhang, R. L., Zhang, Z. G., Wang, Y., LeTourneau, Y., Liu, X. S., Zhang, X., Gregg, S. R., Wang, L. and Chopp, M. (2007). Stroke induces ependymal cell transformation into radial glia in the subventricular zone of the adult rodent brain. *J. Cereb. Blood Flow Metab.* **27**, 1201-1212.